Experiments on Large Cosmic-Ray Bursts under Thick Absorbers at 11,500-Feet Elevation*

THOMAS G. STINCHCOMB
Department of Physics, University of Chicago, Chicago, Illinois
(Received February 13, 1951)

Using a Carnegie Model "C" ionization chamber together with Geiger-Mueller tube coincidence circuits, the nature of the radiation which produces large bursts (greater than 200 particles) of cosmic rays under thick absorbers at 11,500-feet elevation has been investigated at Climax, Colorado. The percentage of this radiation which was accompanied by air showers was determined and found to be dependent upon the burst size. The absorption mean free paths for the burst-producing radiation (excluding bursts produced by μ-mesons and by air showers) were measured in lead and iron and found to be 350 ± 40 g/cm^2 in lead and 240 ± 20 g/cm^2 in iron. The barometric effect on this radiation yielded an absorption mean free path of 65 ± 14 g/cm^2 in the atmosphere, and the zenith angle distribution was found to be that due to an absorption mean free path of 75 ± 14 g/cm^2. These results are shown to indicate that the radiation responsible for these large bursts consists largely of protons and π-mesons of energy greater than 60 Bev.

I. INTRODUCTION

THE problem of the origin of large bursts of cosmic radiation under thick absorbers at mountain elevation has been discussed by several authors.[1-5] They have noted that the rates of occurrence of these bursts are several times higher at mountain elevation than at sea level. It has been generally accepted that at sea level most of these bursts are produced by energetic μ-mesons through bremsstrahlung and knock-on processes.[6] To explain the observed altitude dependence, energetic air showers, nuclear interactions, and bremsstrahlung due to π-mesons and nucleons have been proposed as agencies for production of these bursts at mountain altitude.

Fahy and Schein[3] have found that no appreciable fraction of these bursts at 11,500-feet elevation are actually accompanied by air showers and also that the absorption cross section of this burst-producing radiation in lead is about two times smaller than the geo-

FIG. 1. Diagram showing relative positions of ionization chamber, absorbers, and G-M tubes.

metric cross section of the lead nucleus. These facts indicate that the major portion of the radiation producing large bursts at 11,500-feet elevation is certainly neither μ-mesons nor air showers. Instead, these facts show that this radiation most likely loses its energy in nuclear collisions.[4,5]

It is shown below that the composition of these large bursts is mostly electronic. Consequently, the hypothesis that the bursts are cascade showers produced in nuclear interactions is adopted. This hypothesis is strengthened by the fact[7,8] that, recently, in cloud chambers at this altitude very high energy penetrating showers have been observed which nearly always (90 percent) produce a large shower of electronic radiation also. These electronic showers are often double-cored, and sometimes occur with many cores.

Neutral mesons are known to decay into two γ-rays with a mean lifetime[9] of less than 10^{-13} second. No satisfactory explanation has yet been found for the occurrence of these large cascade showers other than the hypothesis that they are multiple-cored showers produced by the decay of one or more neutral mesons coming from a nuclear collision. Further experimental information regarding the nuclear interaction of the burst-producing radiation has seemed desirable, and it is the purpose of this paper to describe experiments (carried out at Climax, Colorado, elevation 11,500 feet) which were designed to yield such information.

II. EXPERIMENTAL ARRANGEMENT AND TECHNIQUES

The ionization chamber used for these experiments is a Carnegie Model "C" meter.[10] The chamber is a steel sphere of 17.5 cm inside radius, with walls 1.2 cm thick, and it is filled with very pure argon to a pressure of 50 atmospheres. It was mounted concentrically within a
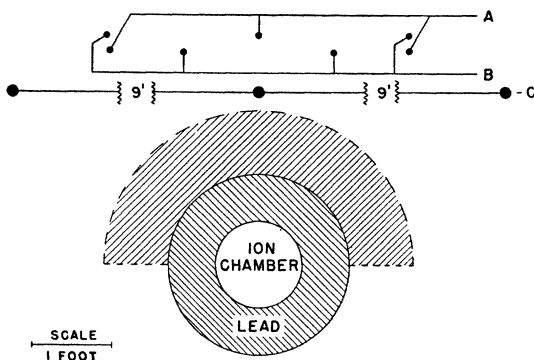
* Assisted by the joint program of the AEC and ONR.
[1] M. Schein and P. S. Gill, Revs. Modern Phys. 11, 267 (1939).
[2] R. E. Lapp, Phys. Rev. 69, 321 (1946).
[3] E. F. Fahy and M. Schein, Phys. Rev. 75, 207 (1949).
[4] H. S. Bridge and B. Rossi, Phys. Rev. 75, 810 (1949).
[5] Y. Fujimoto and S. Hayakawa, Prog. Theor. Phys. 4, 502 (1949).
[6] B. F. Christy and S. Kusaka, Phys. Rev. 59, 414 (1941).

[7] M. B. Gottlieb, Phys. Rev. 82, 349 (1951).
[8] A. J. Hartzler, Phys. Rev. 82, 359 (1951).
[9] Bjorklund, Crandall, Moyer, and York, Phys. Rev. 77, 213 (1950). Steinberger, Panofsky, and Stellar, Phys. Rev. 78, 802 (1950). Panofsky, Aamodt, and York, Phys. Rev. 78, 825 (1950). Carlson, Hooper, and King, Phil. Mag. 41, 701 (1950).
[10] Compton, Wollan, and Bennett, Rev. Sci. Instr. 5, 415 (1934).

steel spherical shell of 3-mm thickness and inside radius 36 cm. The space between the chamber and the shell was filled with lead shot so that there was an equivalent of 10.7 cm of solid lead around the chamber in addition to the chamber walls. This shield is used as a standard shield on all Carnegie Model "C" meters.

In order to obtain data on the absorption of the burst-producing radiation in dense materials, an additional hemispherical sheet-iron shell of 62-cm radius was mounted concentrically over the apparatus. The space between this shell and the inner shell could be filled with lead shot or iron shot to the equivalent thickness of 16-cm solid Pb or 17.3-cm solid Fe. The arrangement is shown in Fig. 1. The spherical symmetry of the geometry of the arrangement is to be noted. Radiation causing bursts in the chamber must penetrate nearly the same amount of absorber no matter at what zenith or azimuthal angle it enters. In order to determine the zenith angle distribution of the burst-producing radiation, a conical iron shield (described in Sec. VI, Fig. 7) was used.

In order to detect events in which bursts were accompanied by air showers, a simple method for recording the air showers was used. Three groups of several Geiger-Mueller counters each were connected in three Rossi type coincidence circuits. Group A consisted of three 2.5-cm by 39-cm counters. Group B consisted of four 2.5-cm by 39-cm counters. Group C consisted of three 5.1-cm by 50-cm counters. The counters were mounted in racks of light material above all the shielding around the chamber. The positions of the counters are shown in Fig. 1.

The Lindemann electrometer, which measures the ionization in the chamber, was grounded every 15 minutes, and every hour a voltage of 0.50 v was applied to it to check its sensitivity. The record of this ionization and of the Geiger-Mueller counter coincidences was obtained by using a camera arrangement. A sample of the record is shown in Fig. 2, illustrating four bursts: (1) greater than 4 mm, (2) greater than 8 mm, (3) greater than 2 mm, and (4) greater than 16 mm. Also shown are: the grounding and checking of the sensitivity of the electrometer, the marks indicating air showers, and similar marks produced artificially one per minute. The apparent coincidences between these latter marks and bursts were, of course, entirely accidental and were used to evaluate the resolving time between any of the marks and a burst. This resolving time was 8 seconds. Using this known resolving time, the recorded coincidences between air showers and bursts were corrected for accidentals in the usual way.

A continuous record of the barometric pressure was obtained by using an aneroid barograph calibrated against a standard mercurial barometer.

The heights of the bursts, d, were noted with the aid of an ordinary magnifying glass and were classified according to whether they were greater than 2 mm, 3 mm, 4 mm, etc., on the paper. Bursts smaller than
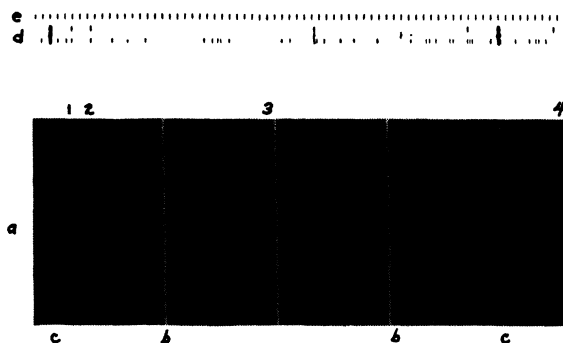

FIG. 2. Sample record showing (a) electrometer trace, (b) grounding of electrometer, (c) sensitivity check, (d) air shower marks, and (e) artificial marks.

2 mm were ignored so that statistical fluctuations in the normal intensity and in the compensation would be eliminated.[11]

A consideration involving the height of the burst was that concerning the effect of the length of time required to record the burst. This "time of rise" could be measured directly from the record and was determined to be 10 seconds and independent of the burst size. If during these 10 seconds the chamber records no net ionization other than that due to the burst, the size of the burst is not affected. On the other hand, if the compensation is not adjusted to an exact null, there will be some net ionization in addition to the burst recorded in the 10-second interval. This will add to or subtract from the real size of the burst according to whether the chamber is under or over compensated. Because of the high sensitivity employed and the relatively large variations in the normal cosmic-ray intensity (due to the large barometric changes at Climax), this effect was found to be not negligible. The slope of the electrometer trace was averaged over each observation period, and the resulting correction was applied to the burst size. This correction varied from zero to 0.1 mm and was important only for the small bursts.

To determine the number of particles which pass through the chamber and produce the observed burst of ionization, a procedure similar to that used by Schein and Gill[1] is followed. The number of ion pairs i in a burst of d mm is

$$i = dc/(300ve) = 0.96d \times 10^7 \text{ ion pairs,}$$

where c is the capacitance of the collecting system of the ionization chamber, the capacitance of which is equal to 95 ± 2 cm; v is the sensitivity of the electrometer which is equal to 68 mm/v; and e is the charge on the electron in esu. For $d = 2$ mm, the bursts must have contained 1.93×10^7 ion pairs. The average amount of energy required to make an ion pair in argon is about 25 ev so that a burst of 2 mm contains about 0.5 Bev

[11] From simple statistical theory, it can be shown that statistical fluctuations producing a deflection of 2 mm are extremely rare (less than one every two months) compared to bursts of 2 mm.
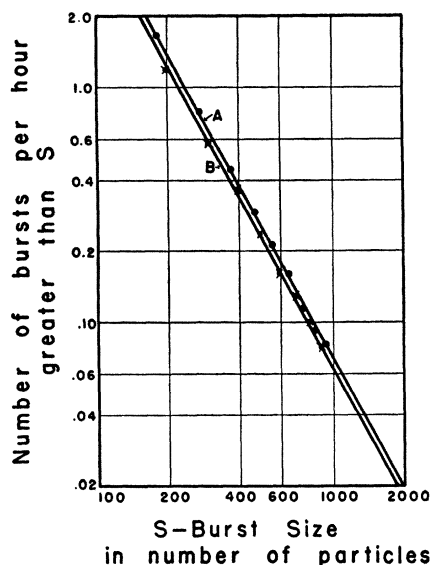
S—Burst Size
in number of particles

Fig. 3. The decrease in burst frequency under 10.7 cm Pb from winter, 1948–49 (curve A, 782.9 hours data, 49.098 cm Hg average barometer) to summer, 1949, (curve B, 590.8 hours data, 49.769 cm Hg average barometer).

of ionization energy. If these were produced mainly by stars, their frequency under 10.7 cm Pb would be very small[12] compared to the frequency observed (about 1.3 per hour). This fact leads one to conclude that the particles producing the ion pairs are not the heavily ionizing star particles but, instead, are minimum ionization particles.

To find the number of ion pairs produced by a minimum ionization particle, one needs to know the average length of path L traversed by the particle going through the chamber and the number g of ion pairs per particle per atmosphere per cm path length. Here L is obtained from the volume V of the chamber by the relation $L = V/\pi r^2$. Since $V = 19.3$ liters, one obtains $L = 20$ cm. The value of g is not known to an accuracy better than 15 percent. The value $g = 96$ ion pairs per particle per atmosphere per cm is chosen, which represents an average of the values used by various investigators. Thus the number S of particles in a burst of d mm is

$$S = i/(50gL) = 100d.$$

Of these, most of the particles must be electrons. Otherwise the total energy of the event would be too large for the observed frequency.

Christy and Kusaka[6] have given a probability function that γ-rays (or electrons) of energy E will develop a cascade shower which will have more than S particles as it passes through the Model "C" ionization chamber. This function indicates that the most probable energy E which will produce a burst of size greater than S is $6\beta S$, where β is 16 Mev for an ionization chamber of

½-inch steel walls surrounded by large thicknesses of lead.[2] Thus, to produce bursts of size greater than 200 particles, γ-rays (or electrons) of energy greater than 2×10^{10} ev will be needed. This would also represent the energy of the burst-producing radiation provided all of its energy goes into the burst. But if the neutral meson hypothesis is adopted, only about $\frac{1}{3}$ of the energy going into meson production can be transferred to the electronic cascade.[9] Then the radiation making the collision in which a burst of 200 particles is produced must have an anergy of 60 Bev or greater.

III. BAROMETRIC EFFECT FOR RADIATION PRODUCING LARGE BURSTS

Preliminary investigations indicated that the frequency of bursts greater than 200 particles under 10.7 cm Pb was about 10 percent greater in winter, 1948–49, than in summer, 1949 (see Fig. 3). Since this was an appreciable change, it was of interest to investigate further the source of the change in order to see if it was caused by the barometric effect, and, if so, to see what the magnitude of the barometric effect is.

For this purpose, an observation period from December, 1949, to April, 1950, was divided into 33 intervals in such a way that the barometric pressure during alternate intervals was above and below the mean pressure p_0 for the whole period, $p_0 = 49.150$ cm Hg. The intervals above p_0 were grouped together and gave a frequency $f_1 = 1.22 \pm 0.04$[13] bursts per hour greater than 200 particles for a total time $t_1 = 884.0$ hours at an average pressure $p_1 = 49.526$ cm Hg. The intervals below p_0 were grouped together and gave a frequency $f_2 = 1.46 \pm 0.04$ bursts per hour greater than 200 particles for a total time $t_2 = 735.8$ hours at an average pressure $p_2 = 48.686$ cm Hg. The burst size *versus* frequency distributions for these two groups are shown in Fig. 4.

Since a slow drift or any other effect producing changes in burst frequency (other than barometric changes) should affect each group in the same way, it should cancel out when comparing the frequencies for the two groups. Thus, the change in frequency between the two groups is assumed to be due to the barometric effect only. For example, a secular increase in burst frequency would increase f_1 by a given factor, but it would increase f_2 by the same factor so that the quantity $(f_1 - f_2)/(f_1 + f_2)$, which is the important quantity in the determination of the magnitude of the barometric effect, would be unchanged.

To determine the magnitude of the barometric effect, one assumes that the barometric variation in the amount of matter above the recording apparatus is small enough so that the relation between the amount of this matter and the intensity of the burst-producing radiation can be assumed to be linear to the first ap-

---

[12] Bridge, Hazen, Rossi, and Williams, Phys. Rev. **74**, 1083 (1948).

[13] Errors are standard statistical errors due to the random occurrence of these events. Errors from all other sources were small compared to statistical errors.

proximation; i.e., that $f = (df/dp)p + k$ where f, p, and k represent the frequency of events, barometric pressure, and a constant, respectively. The assumption is justified because (as will be seen below) the absorption of this radiation is exponential in matter with an absorption mean free path very large compared to the barometric variations.

One can define a barometric coefficient $\alpha = (1/f)df/dp$ which is the fractional change in frequency per unit change in barometric pressure. One then finds that α is given by the formula

$$\alpha = \frac{(\Sigma_i m_i q_i)(\Sigma_i t_i)}{(\Sigma_i q_i^2 t_i)(\Sigma_i f_i t_i)},$$

and that the fractional error in α is given by the formula

$$\frac{\delta\alpha}{\alpha} = \delta m\left[\frac{\Sigma_i q_i^2 t_i}{(\Sigma_i m_i q_i)^2} + \frac{\Sigma_i t_i}{(\Sigma_i f_i t_i)^2}\right]^{\frac{1}{2}},$$

where

$$m_i = f_i t_i - t_i \Sigma_j f_j t_j / \Sigma_j t_j \quad \text{and} \quad q_i = p_i - \Sigma_j p_j t_j / \Sigma_j t_j,$$

where $\delta m = \delta m_i/t_i^{\frac{1}{2}}$, and where f_i, t_i, and p_i refer to the frequency of events, the total time, and the barometric pressure, respectively, during the ith group.

These formulas are derived by a method similar to that employed by Janossy and Rochester.[14] Applying these formulas to the data from December, 1949, to April, 1950, one obtains

$$\alpha_1 = -0.21 \pm 0.05 \text{ per cm Hg pressure.}$$

The burst frequencies during two other observation periods, December, 1948 to January, 1949, and May to June, 1949, can now be examined to ascertain whether or not these changes in burst frequency are due to the barometric effect only (Fig. 3 and Table I).

One can use the barometric coefficient $\alpha_1 = -0.21 \pm 0.05$ per cm Hg together with the burst frequency during the observation period December, 1949 to April, 1950 to determine the burst frequencies expected during the observation periods from December, 1948 to January, 1949, and from May to June, 1949, assuming that all of the changes in burst frequencies were due to the barometric effect. One thus calculates 1.34 ± 0.03 bursts per hour (greater than 200 particles) for December, 1948 to January, 1949, and 1.16 ± 0.04 for May to June, 1949. That these figures agree within experimental error with the observed burst frequencies (Table I) demonstrates that the variations in the burst frequency under 10.7 cm Pb are most likely due only to variations in barometric pressure.

Hence, one can include all data taken under 10.7 cm Pb from December, 1948 through April, 1950, to obtain a better value of the barometric coefficient. When this

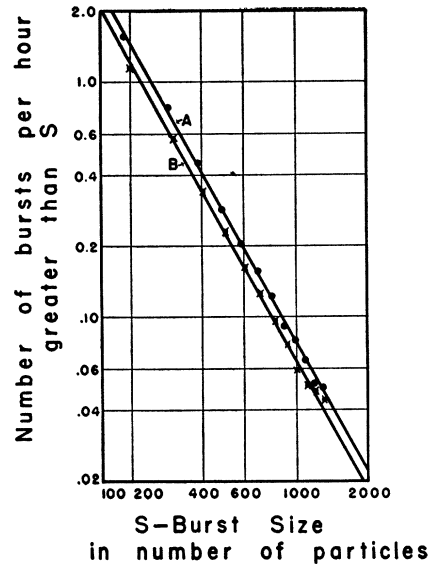[14] Janossy and Rochester, Proc. Roy. Soc. (London) A183, 186 (1944).

FIG. 4. The barometric effect on burst frequency in winter, 1949–1950. Curve A is from 735.8 hours data at average barometer 48.686 cm Hg, and curve B is from 884.0 hours data at average barometer 49.526 cm Hg.

is done, one gets

$$\alpha_2 = -0.18 \pm 0.04 \text{ per cm Hg pressure.}$$

IV. THE EFFECT OF AIR SHOWERS ON BURSTS UNDER THICK ABSORBERS

Before attempting to interpret the data concerning bursts in coincidence with air showers, the accidental coincidences must be considered. The evaluation of the accidental coincidences between bursts and showers was described in Sec. II. All (within statistical error) of the coincidences between bursts and showers which tripped only one of the G-M coincidence circuits, either A, B, or C coincidences, were found to be accidental. Of the coincidences between bursts and showers which tripped two of the three coincidence circuits, the AC and BC coincidences were found to be accidental, while the AB coincidences were found to be nearly all real. Nearly all of the coincidences between bursts and showers which tripped all three of the coincidence circuits were found to be real. Therefore, the events in which bursts occurred along with shower coincidences AB or ABC have been selected and then corrected for

TABLE I. Changes in burst frequency under 10.7 cm Pb. (Here f is the number per hour of bursts greater than 200 particles; p is the average barometric pressure in cm Hg; and $p_0 = 49.150$ cm Hg.)

Observation period	f	p
December, 1948, to January, 1949	1.35 ± 0.04	49.098
May to June, 1949	1.22 ± 0.05	49.769
December, 1949, to April, 1950 pressure greater than p_0	1.22 ± 0.04	49.526
December, 1949, to April, 1950 pressure less than p_0	1.46 ± 0.04	48.686

TABLE II. Bursts accompanied by air showers. (Here N is the total number of bursts of size greater than S; $BABAS$ is the number of bursts of size greater than S which are accompanied by air showers; and S is the size of the burst in number of particles.)

S	10.7 cm Pb only			10.7 cm Pb plus 129 to 136 g/cm Fe		
	N	$BABAS$	percent	N	$BABAS$	percent
200	3206	113	3.5±0.3	2178	61	2.8±0.4
300	1583	70	4.4±0.5	1072	38	3.5±0.6
400	934	49	5.2±0.8	634	26	4.1±0.8
500	607	39	6.4±1.0	412	21	5.1±1.1
600	429	31	7.2±1.3	291	17	5.8±1.4
700	332	26	7.8±1.6	225	14	6.2±1.7
800	251	22	9± 2	170	12	7± 2
1000	169	16	10± 2	115	9	8± 3
1200	120	14	12± 3	81	8	10± 4
1600	79	9	11± 4	54	5	9± 4
2000	51	7	14± 6	34	4	12± 6
2500	31	6	19± 9	21	3	14± 9
3200	22	5	23±12	15	3	20±13
4000	9	5	56±31	6	3	50±33

accidental coincidences using the known resolving time which is 8 seconds (Sec. II, paragraph 4). These events are bursts accompanied by air showers and will be denoted hereafter by $BABAS$.

Table II shows the comparisons between the number of bursts of various sizes and the numbers of these bursts accompanied by air showers. Columns 2, 3, and 4, contain data taken during 2331 hours when both the ionization chamber and the shower detection circuits were operating together and when the ionization chamber was surrounded by the standard spherical 10.7 cm Pb shield only. Columns 5, 6, and 7 contain data taken during 3068 hours when both chamber and shower circuits were operating together and when the chamber was shielded by the standard spherical Pb shield and by 129 to 136 g/cm² of Fe in addition.

It can be seen that the percentage of $BABAS$ does not change appreciably as extra absorber is added. This means that the penetrating component of the air showers is the agent which produced these $BABAS$. If it were the soft component, the percentage of $BABAS$ should be reduced considerably (by a factor of at least 100) when extra absorber of 9 radiation units is present. Thus, these $BABAS$ present evidence that penetrating particles of energies greater than 60 Bev exist in the air showers.

Furthermore it is evident from Table II that the correlation of bursts with air showers increases with increasing burst size. This means that of the total burst-producing radiation the proportion which occurs as part of an air shower increases with increasing burst size. This portion of the radiation must therefore be derived from radiation with energies of a higher order of magnitude.

V. ABSORPTION OF THE BURST-PRODUCING RADIATION IN LEAD AND IRON

The purpose of the following experiments was to measure the absorption of the burst-producing radiation

in large thicknesses of lead and iron. The experiments performed were the following: (A) The measurement of burst frequencies under the standard spherical 10.7 cm Pb shield of the Model "C" meter (see Sec. II); (B) The measurement of burst frequencies under the standard Pb shield plus the additional hemispherical shell filled with lead shot (equivalent to 16.0 cm of solid Pb); (C) The measurement of burst frequencies under the standard Pb shield plus the additional hemispherical shell filled with iron shot (equivalent to 17.3 cm of solid Fe). The results of these experiments (bursts accompanied by air showers were not included) are shown in Table III and in Figs. 5 and 6.

Experiment (A) contains data from a total of 2994.3 hours at an average pressure 49.255 cm Hg during three periods: December, 1948 to January, 1949; May to June, 1949; and December, 1949 to April, 1950. The

TABLE III. Burst frequency under (A) 10.7 cm Pb; (B) 26.7 cm Pb; and (C) 10.7 cm Pb plus 17.3 cm Fe. (Here S is the burst size in number of particles, and $f(S)$ is the number per hour of bursts greater than S.)

(A)		(B)		(C)	
S	$f(S)$	S	$f(S)$	S	$f(S)$
197[a]	1.285±0.022	257[b]	0.518±0.019	199	0.721±0.024
297	0.627±0.015	346	0.298±0.015	299	0.338±0.017
397	0.367±0.012	434	0.194±0.012	399	0.191±0.013
497	0.235±0.010	523	0.134±0.010	499	0.121±0.010
597	0.165±0.008	612	0.091±0.008	599	0.083±0.008
697	0.127±0.007	701	0.062±0.007	700	0.060±0.007
797	0.095±0.006	790	0.045±0.006	800	0.040±0.006
897	0.074±0.006	880	0.035±0.005	900	0.033±0.005
1000	0.064±0.005	970	0.030±0.005	1000	0.030±0.005
1100	0.053±0.005	1060	0.025±0.005	1100	0.022±0.004
1200	0.044±0.004	1230	0.019±0.004	1200	0.019±0.004
1400	0.037±0.004	1410	0.014±0.004	1400	0.010±0.003
1600	0.029±0.006	1590	0.011±0.003	1600	0.006±0.002
2000	0.018±0.003	1950	0.009±0.003	2000	0.004±0.002
2500	0.011±0.002	2480	0.006±0.002	2800	0.002±0.001
3200	0.007±0.002	3190	0.004±0.002	4000	0.001±0.001

[a] The burst sizes used here are not exact multiples of 100 because of the effect of the finite collection time on the number of particles in the burst (discussed in Sec. II).
[b] In experiment (B) the sensitivity of the electrometer was 77 mm per v instead of 68 mm v so that $S = 89d$ instead of $100d$.

burst frequencies from these three periods agree with each other within experimental error when corrected for the barometric effect (see Sec. III). Experiment (B) contains data from 1448.7 hours at an average pressure 49.692 cm Hg during September to November, 1948. Experiment (C) contains data from 1267.2 hours at an average pressure 50.278 cm Hg during June to August, 1949.

In order to carry out the measurements of the absorption of burst-producing radiation, it was necessary to make sure that transition effects did not occur in the extra absorber used. To make sure of this, the standard shield of 10.7 cm Pb (121 g/cm²) was always used. This thickness is well beyond both the peak (at about 4 cm Pb) of the transition curve for large bursts[2,15] and the
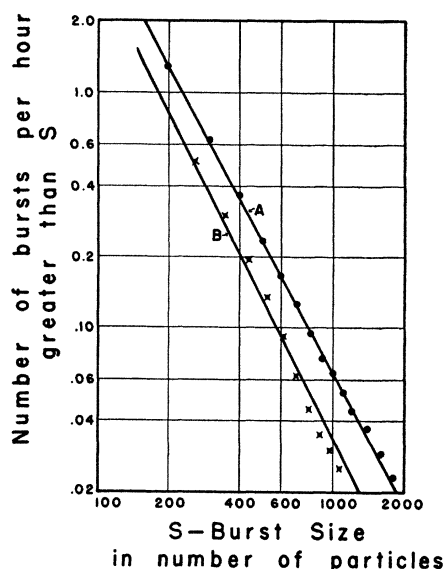
[15] H. Nie, Z. Physik 99, 453 (1936).

FIG. 5. Absorption of burst-producing radiation in 181 g/cm² Pb. Curve A is from 2994.3 hours data under 10.7 cm Pb at average barometer 49.225 cm Hg, and curve B is from 1448.7 hours data under 26.7 cm Pb at average barometer 49.692 cm Hg.
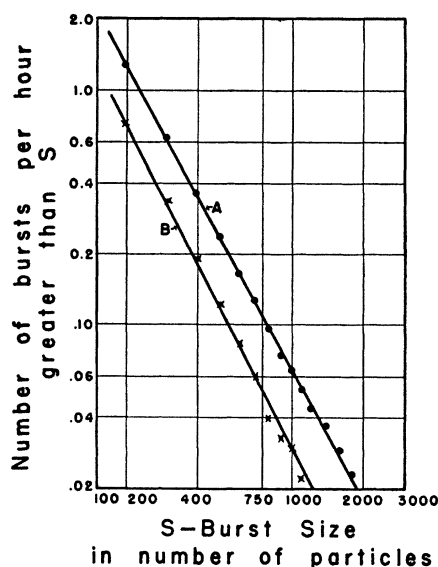

FIG. 6. Absorption of burst-producing radiation in 135 g/cm² Fe. Curve A is from 2994.3 hours data under 10.7 cm Pb at average barometer 49.225 cm Hg, and curve B is from 1267.2 hours data under 10.7 cm Pb plus 17.3 cm Fe at average barometer 50.278 cm Hg.

peak (at about 15 g/cm² Pb) of the transition curve for the nucleonic component which produces stars.[16,17]

The electronic cascades of which these bursts consist obtain their maximum development at 5 to 10 radiation units.[6] Thus, bursts originating at a point in the Pb at a distance above the ionization chamber of 5 to 10 radiation units contribute more to the total number of bursts observed than do bursts originating at other points. Since there are 22 radiation units in the standard spherical shield, the bursts originating in the top of it would by the time they reach the chamber have at least 100 times fewer particles than they had at the maximum. For this reason one considers all the bursts to be produced in the standard spherical shield and none in the additional shielding or in the air above. Consequently, one is measuring the absorption of the burst-producing radiation and not the absorption of the particles in the bursts.

Although the thickness of additional absorber used was 181 g/cm² Pb in experiment (B) and 135 g/cm² Fe in experiment (C), the burst-producing radiation had to traverse a greater thickness unless its path was directed toward the center of the ionization chamber. The determination of the average absorber thickness traversed by this radiation can be carried out, and one finds these average absorber thicknesses to be 188 g/cm² Pb in experiment (B) and 140 g/cm² Fe in experiment (C) (a correction of 4 percent).

Table IV gives the absorption in lead and iron for the various ranges of burst sizes. The barometric coefficient $\alpha_2 = -0.18$ per cm Hg pressure (see Sec. III) was used

[16] J. J. Lord and M. Schein, Phys. Rev. 75, 1956 (1949).
[17] G. Cortini and A. Manfredini, Nature 163, 991 (1949).

in correcting the burst frequencies for the barometric effect. Table IV shows clearly that the absorption of the burst-producing radiation is much too large to be accounted for in terms of the expected absorption of μ-mesons of an energy greater than 2×10^{10} ev. The frequency of such bursts produced by μ-mesons should not have been reduced by more than about 3 percent (due to ionization loss in the absorber). This fact shows conclusively that the major portion of the burst-producing radiation consists of particles different from μ-mesons.

However, it is certain that at least some fraction of the bursts at Climax are produced by μ-mesons, by means of the same mechanism as at sea level. It is worthwhile then to estimate the number of these that occur per hour at Climax. If one lets u be equal to this number, one finds that $(1.27 - u) \exp\{\alpha_2(p_a - p_b)\}$ is the number ν of bursts per hour other than μ-meson-produced bursts which should occur in the same ionization chamber at sea level assuming the absorption to be exponential and assuming that there is no appreciable change in the barometric coefficient α_2 (see Sec. III) between Climax and sea level. (Here p_a and p_b are the barometric pressures at sea level and Climax, respec-

TABLE IV. Absorption of burst-producing radiation in lead and iron. (Here S is the burst size in number of particles; and f_A, f_B, f_C are the burst frequencies for experiments (A), (B), and (C), respectively.)

S	$S > 200$	$200 < S < 400$	$400 < S < 1000$	$1000 < S < 2000$
f_A/f_B	1.46±0.06	1.41±0.07	1.56±0.13	1.68±0.37
f_A/f_C	1.50±0.05	1.46±0.06	1.58±0.12	1.71±0.34

TABLE V. Absorption of burst-producing radiation other than μ-mesons in lead and iron. (Here x_0 is the absorption mean free path in g/cm^2; x_0 in Pb$=(188)/(\ln f_A-\ln f_B)$, x_0 in Fe$=(140)/(\ln f_A-\ln f_C)$, other symbols are the same as for Table IV.)

S	S>200	200<S<400	400<S<1000	1000<S<2000
f_A/f_B	1.71±0.10	1.63±0.11	1.84±0.23	2.02±0.66
x_0 in Pb	350±40	390±60	310±70	270±120
f_A/f_C	1.82±0.11	1.76±0.12	1.96±0.25	2.15±0.69
x_0 in Fe	240±20	250±30	210±40	180±80

tively, and 1.27±0.02 is the total number—excluding bursts accompanied by air showers—of bursts per hour greater than 200 particles, at Climax.) The number ν is equal to 0.011–0.009u burst per hour. In a similar ionization chamber identically shielded at sea level (Cheltenham, Maryland), the burst frequency for bursts greater than 200 particles was found to be 0.16±0.005 burst per hour.[2] From accurate com-

Top View

Front View

14.7° + 14.7°
21.2° + 21.2°
28.0° + 28.0°

A = 17.5 cm
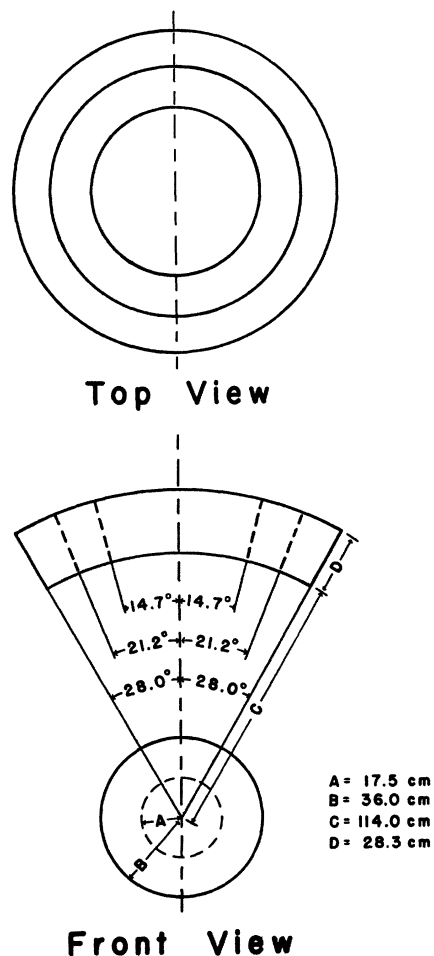B = 36.0 cm
C = 114.0 cm
D = 28.3 cm

FIG. 7. The special shield for measuring the zenith angle dependence of burst-producing radiation. The shield (D) is the volume between two concentric spheres cut by a conical surface with apex at the center of the spheres; the shield is shown in its position relative to the ionization chamber (A) and the 10.7 cm Pb shield (B).

parisons[18] between the chambers, one knows that the chamber used for these experiments would have registered 0.29±0.02 burst per hour greater than 200 particles.

The difference between these 0.29 burst per hour and the number ν must be due to μ-mesons. The probability for the decay of μ-mesons of energy greater than 4×10^{10} ev in 3500 meters is less than 1 chance in 150. (The figure 4×10^{10} ev is chosen, because μ-mesons transfer on the average about $\frac{1}{2}$ their energy to the electronic cascade.[6]) On the other hand, these μ-mesons lose about 3 percent of their energy by ionization loss in the 3500 meters between Climax and sea level. Because the frequency versus size distribution for large bursts is very close to an inverse square law,[2] the number of bursts greater than 200 particles produced by μ-mesons would be 6 percent greater at Climax than at sea level. As a result $u=1.06(0.29\pm0.02-\nu)$ or $u=0.30\pm0.02$ bursts per hour greater than 200 particles produced by μ-mesons at Climax.[19]

Subtracting the frequencies of bursts due to μ-mesons from all the observed frequencies, one finds the absorption of the remainder of the burst-producing radiation. Table V shows these results together with the absorption mean free paths x_0 derived from these results.

The absorption mean free path x_0 bears an inverse relation to the absorption cross section σ_A; namely, $x_0=A/(\sigma_A N_A)$, where N_A is Avogadro's number, and A is the atomic weight of the absorber. In order to see how the absorption cross sections for iron and lead compare, one notes that the ratio of the experimental absorption mean free path in iron (μ-meson bursts excluded) to that in lead is 0.68±0.09. The ratio of the atomic weight of iron to that of lead is 0.27, and 0.68 ±0.09= $(0.27)^{0.29\pm0.10}$. Thus, one can say that the absorption mean free paths are proportional to the 0.29 ±0.10 power of the atomic weight. Consequently, the absorption cross sections are proportional to the 0.71 ±0.10 power of the atomic weight. That the ratio of the absorption cross sections is $A^{\frac{2}{3}}$ within experimental error lends strong support to the hypothesis that the

[18] These comparisons were carried out through the cooperation of Dr. S. E. Forbush of the Carnegie Institution of Washington, D. C. The chamber used for these experiments was compared to a similar chamber maintained by the Carnegie Institution in the Climax laboratory. From direct comparisons between the burst frequencies in the two chambers, the former was found to be 0.92±0.05 times as sensitive as the latter. The latter chamber was then found to be 1.47 times more sensitive than the Cheltenham meter by comparisons made at Cheltenham using a radium source. Thus, the chamber used in these experiments is 1.35±0.06 times more sensitive than the Cheltenham chamber. This means that a burst which would appear to be a 200-particle burst in the Cheltenham chamber would appear to be a 270-particle burst in the chamber used in these experiments. Because the frequency versus size distribution for large bursts at sea level is very close to an inverse square law (reference 2), the number of bursts observed is in a ratio $(200/270)^2=(0.16/0.29)$.

[19] If the value of α_2 has been assumed to be -0.13 per cm Hg which corresponds to an absorption mean free path in the atmosphere of 125 g/cm^2 (see Sec. VI), u would have been equal to 0.27μ-meson bursts per hour at Climax.

burst-producing radiation is absorbed by collisions with nuclei.

The geometrical cross section of a nucleus is given approximately by the formula $\sigma_G = \pi(1.4\times10^{-13})^2 A^{\frac{2}{3}}$. If one assumes that the collision cross section is equal to the geometrical cross section, one calculates that the collision mean free paths are 160 g/cm² and 100 g/cm² for lead and iron, respectively. It is seen that the absorption mean free paths are roughly twice these values, so that it takes an average of about two successive nuclear collisions to absorb the energy of the burst-producing radiation in lead and iron. This fact indicates that in iron and lead successive collisions occur each producing large electron showers. This process is directly observed in cloud chambers.[8]

One should note that experiment (A) gives for the integral burst frequency *versus* size distribution the following relation (at Climax under 10.7 cm Pb and at 49.255 cm Hg pressure): $f = (1.28\pm0.02)(S/200)^{-1.9\pm0.1}$ bursts per hour greater than S particles (excluding air showers but including μ-meson bursts).

VI. THE ABSORPTION OF THE BURST-PRODUCING RADIATION IN THE ATMOSPHERE ABOVE 11,500 FEET

It is of interest to see if the absorption mean free path in the lower part of the atmosphere above Climax is as different from the collision mean free path, 67 g/cm² (corresponding to the geometrical cross section) as it is in iron and lead. Although the absorptions of the radiations which produce stars and penetrating showers show an absorption mean free path of roughly twice the collision mean free path (penetrating showers,[20] 140 g/cm²; proton produced stars,[21] 145 g/cm²), it is worthwhile to find out whether the high energy radiation which produces these large bursts shows the same absorption.

One can deduce the value of the absorption mean free path in the atmosphere above Climax from the value of the barometric coefficient. However, the frequencies of bursts due to μ-mesons must be subtracted from the burst frequencies, just as in Sec. V. This can be done by reducing the burst frequencies in column 3 of Table I by 0.3 per hour. Applying the formulas for the barometric coefficient to these reduced frequencies, one obtains the value

$$\alpha_3 = -0.23\pm0.05 \text{ per cm Hg pressure.}$$

Here α is related to the burst frequency f by the equation

$$\alpha = (13.6/f)df/dx,$$

where x is the depth below the top of the atmosphere in g/cm², and 13.6 is the conversion factor between g/cm² and cm Hg (see Sec. III). The burst frequency as a

[20] T. G. Walsh and O. Piccioni, Phys. Rev. **80**, 619 (1950).
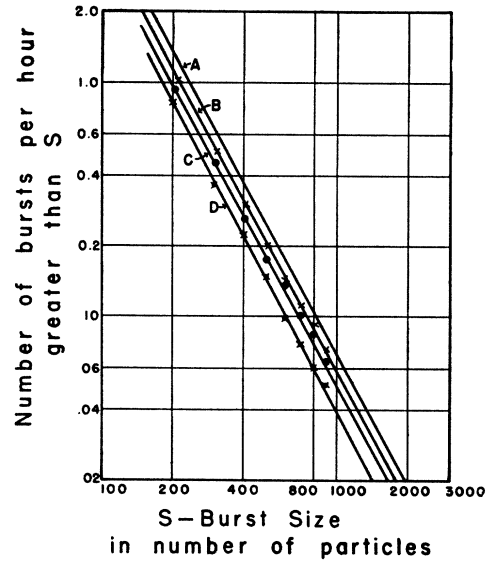[21] J. J. Lord, Phys. Rev. **81**, 901 (1951).

FIG. 8. Burst frequencies under 10.7 cm Pb plus a shield of 136 g/cm² Fe covering zenith angles up to 15.3° (B), 21.6° (C), and 28.3° (D), compared to those under 10.7 cm Pb alone (A).

function of x is given by

$$f(x) = k\int_0^{\pi/2} \exp[-(x/x_0)\sec\theta]\sin\theta\,d\theta,$$

where k is a constant. Carrying out the differentiation, one can show that[22]

$$1/x_0 = -[(\alpha/13.6)+(1/x)]$$

if one assumes that x is large compared to x_0. At Climax, $x = 675$ g/cm², so one obtains for the absorption mean free path in the atmosphere above Climax from the barometric effect

$$x_0 = 65\pm14 \text{ g/cm}^2.$$

The zenith angle dependence of the burst-producing radiation was next investigated in order to determine whether this radiation is as sharply collimated in the vertical direction as is indicated by this large value of the absorption mean free path in the atmosphere.

A special shield was used to determine the zenith angle dependence of the burst-producing radiation and is shown in Fig. 7. When filled with iron shot, the shield is 136 g/cm² thick. This thickness when averaged over all possible paths through the shield and ionization chamber is found to be increased by a factor 1.005 which is quite negligible. The zenith angles (at the center of the ionization chamber) covered by the three sections of the shield were measured and found to be 14.7°, 21.2°, 28.0°. When these angles are averaged over all possible paths through the ionization chamber, they are found to be 15.3°, 21.6°, and 28.3°.

[22] The term $1/x$ contains the correction due to the Gross transformation. It can be seen that this correction amounts to about 10 percent.

TABLE VI. The zenith angle dependence of burst-producing radiation. (Here θ is the zenith angle covered by the shield; $F(\theta)$ is the fraction of radiation at zenith angles larger than θ; f_B and f_A are the number of bursts per hour greater than 200 particles with the shield and without the shield, respectively, μ-meson bursts excluded; f_A has been corrected for the difference in barometric pressure.)

θ	f_B	f_A	$F(\theta)$
15.3°	0.83±0.03	0.97±0.02	0.67±0.08
21.6°	0.67±0.03	0.86±0.02	0.49±0.08
28.3°	0.53±0.03	0.81±0.02	0.21±0.08

The experimental results are shown in Fig. 8. Curve A is Fig. 5 (curve A) repeated to show the burst frequency with only the standard Pb shield used. Curves B, C, and D give the frequencies under this standard shield plus the special Fe shield filled to the zenith angles 15.3°, 21.6°, and 28.3°, respectively. Curve B was obtained from 1137 bursts observed in 1123.1 hours during April and May, 1950, at an average barometric pressure of 49.556 cm Hg; curve C from 801 bursts observed in 887.9 hours during June and July, 1950, at an average barometric pressure of 50.078 cm Hg; and curve D from 792 bursts observed in 1081.7 hours during July and August, 1950, at an average barometric pressure of 50.268 cm Hg.

From this figure one obtains for the number per hour of bursts of 200 particles and greater, frequencies per hour of 1.13, 0.99, and 0.78 for curves B, C, and D, respectively. Subtracting the 0.3 burst per hour due to μ-mesons (which are not appreciably absorbed by this special shield), one finds frequencies per hour of 0.83, 0.69, and 0.48 for the shield angles 15.3°, 21.6°, and 28.3°, respectively. These frequencies are to be compared with that from curve A which first has to be corrected for barometric variations and then for μ-meson bursts. Of interest then is the fraction $F(\theta)$ of the radiation entering the apparatus at zenith angles larger than θ. This fraction is a convenient measure of the zenith angle distribution. The fraction entering the shield is

FIG. 9. Plot of $F(\theta)$ sec²θ versus sec$\theta-1$, showing that $F(\theta)$ sec²$\theta=$exp$(1-$sec$\theta)(9.0\pm1.6)$. The upper, middle, and lower curves are exp7.4$(1-$sec$\theta)$, exp9.0$(1-$sec$\theta)$, and exp10.6$(1-$sec$\theta)$, respectively.

$1-F(\theta)$, and of this $\{1-F(\theta)\}$ exp$(-137/240)$ passes through the shield. Thus, the burst frequency with the shield is less than without the shield by a factor

$$F(\theta)+\{1-F(\theta)\} \exp(-137/240)=0.565+0.435F(\theta).$$

Table VI shows the computation of $F(\theta)$.

In order to determine the absorption mean free path from the zenith angle distribution, one notes that the fraction $F(\theta)$ of radiation at zenith angles larger than θ can be written as

$$F(\theta)=\frac{\displaystyle\int_{\theta}^{\pi/2} \exp[-(x/x_0) \sec\theta] \sin\theta d\theta}{\displaystyle\int_{0}^{\pi/2} \exp[-(x/x_0) \sec\theta] \sin\theta d\theta}$$

if one assumes exponential absorption. One can then show that

$$F(\theta) \sec^2\theta=\exp\{(x/x_0)(1-\sec\theta)\}$$

if secθ is not very different from unity and if x/x_0 is large compared to unity. These approximations are justified, since x for Climax is 675 g/cm² and since sec 28.3° $=1.138$. If now one plots $F(\theta)$ sec²θ versus sec $\theta-1$ on semilogarithmic graph paper (Fig. 9), one finds the relation

$$F(\theta) \sec^2\theta=\exp\{(9.0\pm1.6)(1-\sec\theta)\}.$$

Thus, $x_0=75\pm14$ g/cm².[23]

This value of the absorption mean free path of the burst-producing radiation in the atmosphere above Climax is in good agreement with the value 65 ± 14 g/cm² determined from the barometric effect. The collision mean free path (determined from the geometric cross section of the air nucleus) is 67 g/cm². Thus, the absorption mean free path in the atmosphere is almost equal to this collision mean free path. This is also in agreement with the absorption mean free path in the atmosphere of the radiation producing very high energy (E greater than 15 Bev) penetrating showers.[24]

Since no radiation can be absorbed faster than the primary radiation, the primary radiation which produces these large bursts (either directly or indirectly through the agency of secondary radiation) must have an absorption mean free path in the atmosphere not greater than about 70 g/cm². On the other hand, since this absorption mean free path cannot be less than the collision mean free path and since the nuclear collision cross section cannot be appreciably larger than the geometrical cross section of the nucleus, the absorption mean free path for the primary radiation responsible for these large bursts cannot be much less than 67 g/cm².
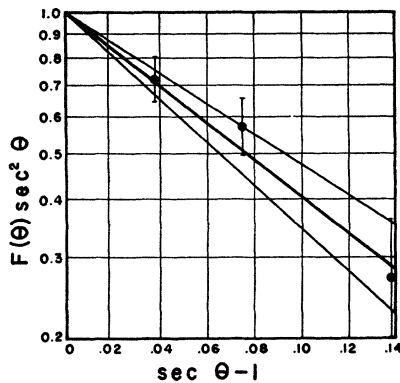
---

[23] The coefficient of $(1-$sec$\theta)$ would have to be 4.8 instead of 9.0 in order to give a value of $x_0=140$ g/cm². The value 9.0 agrees with that given by Gottlieb (reference 7); who obtained an angular distribution for the radiation which produces very high energy penetrating showers corresponding to about cos⁹θ.

[24] Gottlieb, Hartzler, and Schein, Phys. Rev. **79**, 741 (1950).

One therefore concludes that this primary radiation has an absorption mean free path of about 70 g/cm².

Types of secondary radiation which might exhibit this large absorption at these high energies are π-mesons, protons, and neutrons. Neutrons can be eliminated from consideration because of the evidence that nuclear interactions causing electron showers (observed in a cloud chamber) large enough to be bursts are largely (81 percent) caused by ionizing particles.[24] Thus, it seems that the burst-producing radiation (other than μ-mesons and air showers) must consist of very high energy protons (primary or secondary) and/or of π-mesons produced by them.

The probability that secondary radiation generated in the atmosphere produces a large portion of these bursts is small, since this would lead to an absorption mean free path longer than the collision mean free path. On the other hand, the probability that secondary radiation generated in the lead and iron absorber produces a large portion of the bursts is large, since the absorption mean free paths for lead and iron are about twice the collision mean free paths. This increased probability may be due to the possibility that several π-mesons can interact simultaneously in the burst-producing region of the absorber and produce a burst in the ionization chamber which is several times larger than a burst produced by one π-meson alone. This means that the average energy of the successive collisions may not be attenuated as fast in the absorber as it is in the atmosphere. The increased probability may also be due to the absence of the decay of π-mesons in lead and iron.

The Microwave Absorption Spectrum of Nitrosyl Chloride NOCl*

JOHN D. ROGERS, WILLIAM J. PIETENPOL, AND DUDLEY WILLIAMS
Mendenhall Laboratory of Physics, Ohio State University, Columbus, Ohio
(Received April 2, 1951)

The absorption spectrum of nitrosyl chloride has been studied in the region between 21,000 and 23,000 mc/sec. Eight groups of closely spaced absorption lines have been observed; thirty-one individual lines have been resolved. The main features of the observed spectrum can be satisfactorily explained in terms of the rotational transition $J=1 \rightarrow 2$ for molecules in the ground and lowest excited vibrational state; the observed hyperfine-structure is satisfactorily explained in terms of nuclear quadrupole interactions involving the chlorine nuclei. The rotational constants for molecules in the ground vibrational state are: for $NOCl^{35}$, $A=2.845$, $B=0.19141$, and $C=0.17934$ cm^{-1}; for $NOCl^{37}$, $A=2.854$, $B=0.18682$, and $C=0.17534$ cm^{-1}. Values for the quadrupole interaction terms are given. The ratio Q^{35}/Q^{37} obtained in this study was 1.34 ±0.08.

ELECTRON diffraction studies[1] of nitrosyl chloride have yielded the following values for interatomic distance and bond angle: $d(N-Cl)=1.95\pm0.01\times10^{-8}$ cm; $d(N-O)=1.14\pm0.02\times10^{-8}$ cm; $d(O-Cl)=2.65\pm0.01\times10^{-8}$ cm; angle ONCl$=116°\pm2°$. From these values and from the known masses of the nitrogen, oxygen, and chlorine atoms, it is possible to calculate approximate values for the principal moments of inertia of the NOCl molecule. These calculated values are: $I_A=8.82\times10^{-40}$ g·cm², $I_B=149\times10^{-40}$ g·cm², $I_C=158\times10^{-40}$ g·cm²; and the corresponding rotational constants are: $A=3.17$ cm^{-1}, $B=0.188$ cm^{-1}, $C=0.177$

---

[1] J. A. A. Ketelaar and K. J. Palmer, J. Am. Chem. Soc. **59**, 2629 (1939).

cm^{-1}. These values indicate that NOCl is, to a close approximation, a *prolate symmetric molecule.*

Treating NOCl as a symmetric molecule for which the centrifugal stretching can be neglected and assuming the dipole moment to lie principally along the unique axis, one would expect the frequencies in the rotational spectrum to be given by the expression

$$\nu=(B+C)(J+1),$$

which predicts absorption lines in the vicinity of 0.366 cm^{-1}, 0.732 cm^{-1}, and 1.09 cm^{-1} for lower J values of 0, 1, and 2, respectively. The predicted 0.732-cm^{-1} line falls in a spectral region for which microwave oscillator tubes are readily available. Therefore, the microwave absorption spectrum of NOCl was studied in this region in the hope of observing absorption lines associated with the transition $J=1$ to $J=2$.

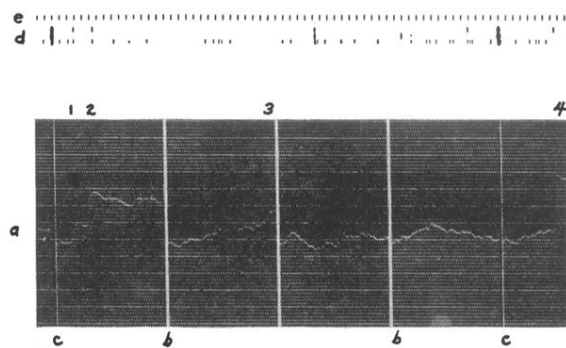In the study of the absorption spectrum, the re-

FIG. 2. Sample record showing (a) electrometer trace, (b) grounding of electrometer, (c) sensitivity check, (d) air shower marks, and (e) artificial marks.